# Molecular Signatures and Resistance Mechanisms in Chronic Lymphocytic Leukemia and Mantle Cell Lymphoma

Ph.D. thesis

**Tamás László, MD**

Semmelweis University Doctoral School

Pathological and Oncological Division

**Supervisor:** Csaba Bödör, DSc.

**Official reviewers**: Zoltán Wiener, MD, DSc

Károly Szuhai, MD, PhD

**Head of the Complex Examination Committee:**

Attila Tordai MD, DSc

**Members of the Complex Examination Committee:**

Péter Attila Király, MD, PhD

Zoltán Wiener, MD, DSc

Budapest, 2025

## *1. INTRODUCTION*

B-cell lymphomas constitute 85-90% of all non-Hodgkin lymphomas, with chronic lymphocytic leukemia/small lymphocytic lymphoma (CLL/SLL) and mantle cell lymphoma (MCL) accounting for roughly 7% and 3-10% of B-cell lymphomas, respectively. These two entities show remarkable similarities in their molecular development, as well as in prognostication and treatment strategies.

*TP53* deficiency (the presence of a mutation or the deletion of the short arm of chromosome 17) represents the most important prognostic and predictive biomarker in both entities. Recent NGS studies identified low-burden (mutations restricted to a subpopulation of the tumour cells with variant allele frequencies (VAFs) far below the sensitivity of Sanger sequencing) *TP53* mutations in 5–35% of CLL patients. According to the most recent studies, low-burden *TP53* mutations seem to negatively impact overall survival (OS), nevertheless, it is becoming clear that these results must be contextualized within the framework of disease stage and therapeutic approach. Despite the introduction of novel treatment modalities and *TP53* deficiency still remains the major prognostic/predictive biomarker in CLL and MCL.

In the last decade, the introduction of targeted agents such as Bruton's tyrosine kinase inhibitors (BTKi) or the pro-apoptotic venetoclax has revolutionized the treatment of both CLL and MCL. Despite the remarkable clinical results, resistance may occur in both CLL and MCL, conferring a dismal prognosis. Despite the similarities between CLL and MCL, resistance mechanisms to ibrutinib or venetoclax appear to differ, with CLL being characterized by acquired resistance mutations, while primary resistance being more common in MCL. Although the genetic landscape of MCL is increasingly well defined, the molecular background of resistance mechanisms are still unclear. Recently several studies focused on the molecular background of BTKi resistance, however only a handful of data is available regarding venetoclax resistance.

## 2. *OBJECTIVES*

In my PhD. work we aimed the following specific objectives:

- To scrutinize the occurrence and architecture of low-burden *TP53* mutations in CLL, using a high-sensitivity NGS-based method

- To establish a reliable and reproducible threshold for NGS-based *TP53* variant calling

- To assess the clinical impact of low-burden *TP53* mutations, with special emphasis on their prognostic value in the context of the IGHV status

- To study the copy number profile of MCL patients treated sequentially with BTKi and venetoclax using low-coverage whole genome sequencing

- To improve our limited understanding of clonal evolution and resistance mechanisms associated with BTKi and venetoclax in MCL

## 3. *MATERIALS AND METHODS*

Peripheral blood samples from 901 patients with CLL were collected across 20 oncohematology units in Hungary. In the MCL cohort, 21 formalin-fixed, paraffin-embedded (FFPE) tissue samples were examined from 12 patients. During the processing of peripheral blood samples, genomic DNA was extracted after Ficoll/Histopaque density-gradient cell separation in all cases. The proportion of CLL cells in each sample was determined by flow cytometry. Genomic DNA was extracted using the MagCore Nucleic Acid Extraction Kit (RBC Bioscience, Taipei, Taiwan) or the High Pure PCR Template Preparation Kit (Roche, Mannheim, Germany) according to the manufacturer's instructions. During the processing of FFPE samples, DNA was extracted using the QIAamp DNA FFPE Tissue Kit (Qiagen, Hilden, Germany) according to the manufacturer's instructions. Both peripheral blood and FFPE-derived genomic DNA

were quantified using Qubit HS dsDNA Kit (Thermo Fisher Scientific, Waltham, MA, USA).

*TP53* sequencing was performed using the Multiplicom SureMASTR *TP53* Panel (Agilent, Santa Clara, CA, USA), which covers the entire coding sequence of the *TP53* gene. Libraries were prepared according to the manufacturer's instructions. Data processing and analysis were conducted using Sequence Pilot 5.1.0 (JSI Medical Systems, New York, NY, USA). *TP53* coding-region variants were annotated using the *TP53*-specific UMD_TP53 (Universal Mutation Database, Seshat), the *TP53* Database, and the COSMIC database. Variants with a variant allele frequency (VAF) below 10% were classified as low burden, while those with VAF ≥10% were considered high burden. All low-burden variants, along with 33.6% (37/110) of the high-burden mutations, were confirmed by either NGS or droplet digital polymerase chain reaction (ddPCR). Low-burden variants were validated using an alternative *TP53* NGS panel (CleanPlex, Paragon Genomics, Fremont, CA, USA). *TP53* analysis on MCL FFPE samples was carried out using the CleanPlex *TP53* panel.

Validation of selected *TP53* variants (R196, Y220C, R248W, R248Q, Y234C) was performed using droplet digital PCR (ddPCR) with custom assays. PCR was performed on a QX200 Droplet Digital PCR system (Bio-Rad Laboratories, Hercules, CA, USA) according to the manufacturer's instructions, using 100 ng of input DNA. Fractional abundance (FA) was determined as the ratio of droplets containing mutant DNA (a) to the total droplets containing mutant (a) plus wild-type (b) DNA molecules, calculated as $FA = a/(a + b)$.

Immunoglobulin heavy chain (IGH) gene rearrangement and somatic hypermutation analyses were carried out as described by Agathangelidis et al, using consensus IGH gene-specific 3' primers as well as subgroup-specific Leader, FR1, or FR2 primers. DNA amplification with Leader/FR1/FR2 primers was performed by Sanger sequencing, and the data were analyzed utilizing IMGT V-QUEST. CLL samples were analyzed using Leader or FR1 primers, while FR1 or FR2 primers were used on FFPE samples.

The integrity of isolated DNA from FFPE samples was determined using a multiplex GAPDH PCR method, and DNA damage generated

by formalin fixation was repaired utilizing the NEBNext FFPE DNA Repair Kit (New England Biolabs, Ipswich, MA, USA). Low-coverage whole genome sequencing was carried out using the NEBNext Ultra II DNA Library Prep Kit for Illumina, along with NEBNext Unique Dual Index UMI Adaptors (New England Biolabs). Samples exhibiting low integrity underwent amplification with two additional PCR cycles. Individual libraries were pooled equimolarly and sequenced on a NextSeq2000 (Illumina, San Diego, CA, USA) instrument using P2 or P3 flow cell with 50-cycle single-read chemistry.

Survival analysis was carried out using Kaplan-Meier curves and the Log-rank test with GraphPad Prism 8.0.2 (GraphPad Software, San Diego, CA, USA). Overall survival (OS) was calculated from the date of death or last follow-up. Treatment-free survival (TFS) was calculated from the time of first treatment, death from any cause, or last follow-up. Time to first treatment (TTFT) was calculated from sample collection to treatment initiation or last follow-up. Categorical variables were compared by Fisher's exact test. p-values equal to 0,05 or below were considered statistically significant.

# *4. RESULTS*

## *4.1. Molecular screening of TP53 mutations in CLL*

### *4.1.1 Frequency of TP53 mutations*

Using NGS, we identified a total of 225 *TP53* mutations in 17.5% of patients (158/901), with an average variant allele frequency (VAF) of 22.99% (range: 1.0–92.0%) (Figure 1). Among these, 48% (n=109) were classified as high-burden mutations, while 52% (n=116) were low-burden. Multiple *TP53* mutations were found in 28.5% (45/158) of mutated cases, with an average of 2.5 mutations per patient (range: 2–5). Low-burden *TP53* mutations occurring alone were detected in 39% (62/158) of all mutated cases, with 82.3% (51/62) of these having a single low-burden mutation. The prevalence of patients carrying only low-burden *TP53* mutations was 4%, 6%, and 13% in diagnostic, pre-treatment, and post-treatment samples, respectively (Figure 1).

Sole high-burden *TP53* mutations were identified in 44% (69/158) of mutated patients, while 17% (27/158) harbored both high- and low-burden mutations (Figure 1).

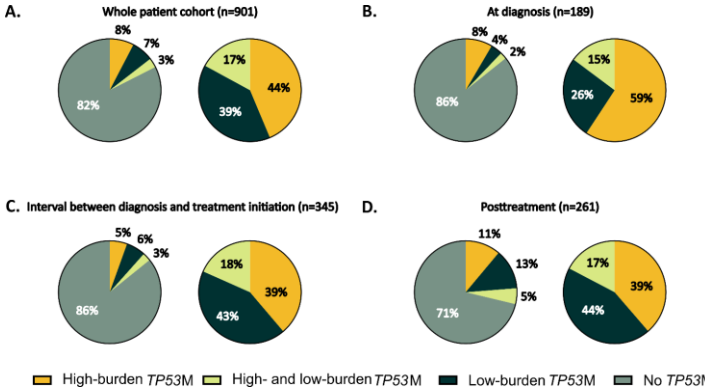


***Figure 1. Frequency and distribution of TP53 mutations. (***A) *TP53* mutation was identified in 17.5% of the patients with the illustratedfrequency and distribution of low-burden and high-burden mutations. (B–D) The frequency and distribution of *TP53* mutations in samples collected at the time of diagnosis, before treatment initiation, and post-treatment respectively. Abbreviation: M, mutation

### *4.1.2. Determination of a reliable and reproducible cut-off value for TP53 variant reporting*

Across the full patient cohort, 68% (153/225) of identified *TP53* variants underwent independent validation, which included all low-burden variants (n = 116) and 33.9% (37/109) of high-burden variants. Of the variants re-tested, 85.0% (153/180) were successfully confirmed. Only validated low-burden variants were included in the study. All high-burden *TP53* mutations going through the re-evaluation process were validated (n = 37), while 81.1% (116/143) of low-burden variants were confirmed. All low-burden *TP53* mutations

with a VAF between 5% and 10% were validated (n = 38), whereas 74.3% (78/105) of variants with a VAF below 5% could be confirmed (Figure 2). Among *TP53* variants with VAF between 2% and 5% (≥2% and <5%; n = 47), 96% (45/47) were validated, using either NGS (n = 39) or ddPCR (n = 6). In contrast, only 57% (33/58) of variants with VAF below 2% were successfully confirmed (Figure 2).

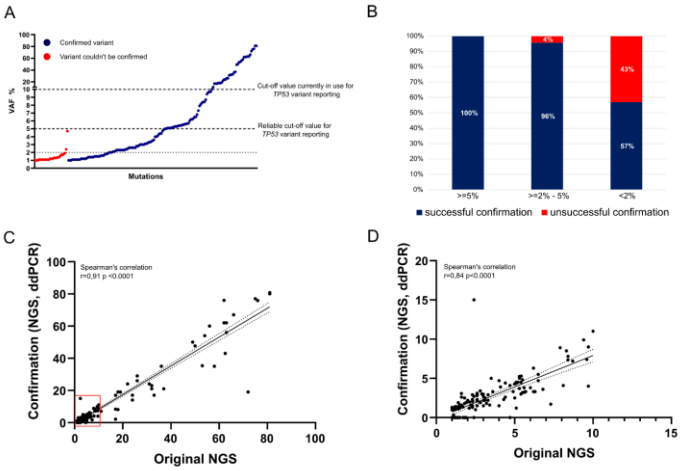


***Figure 2. Graphical representation of the variant allele frequencies of TP53 mutations detected with NGS.*** (A.) Variant allele frequencies of the mutations represent the VAF of their first detection. Blue dots indicate mutations successfully confirmed by NGS or ddPCR, while red dots represent mutations that could not be validated. (B) Distribution of *TP53* mutations with confirmed or unconfirmed status across different VAF groups. (C) Spearman's correlation between VAFs obtained from the original NGS and those from the second NGS or ddPCR during validation. (D) Spearman's correlation between original NGS VAFs and those from the second NGS or ddPCR in samples with initial VAFs below 10% (highlighted in red in panel C). (Abbreviation: VAF, variant allele frequency).

### *4.1.3. Types and distribution of TP53 mutations*

*TP53* mutations were predominantly missense substitutions (74.7%; 168/225), followed by insertions or deletions (indels, 15.6%; 35/225), nonsense mutations (6.2%; 14/225), and splice site variants (3.6%; 8/225) (Figure 3). Missense mutations frequently involved classical hot-spot codons affected by single base substitutions, leading either to „DNA-contact mutants" (residues 248 and 273; 29/225, 12.9% of all TP53 variants) or to „conformational mutants" (residues 175, 245, 249, and 282; 20/225, 8.9% of all variants). Among indel mutations, 25.7% (9/35) affected codon 209 through a two-nucleotide deletion (c.626_627del), a lesion highly characteristic of CLL. In terms of localization, 93.8% (211/225) of mutations were found within the DNA-binding domain (residues 94–292) (Figure 3).

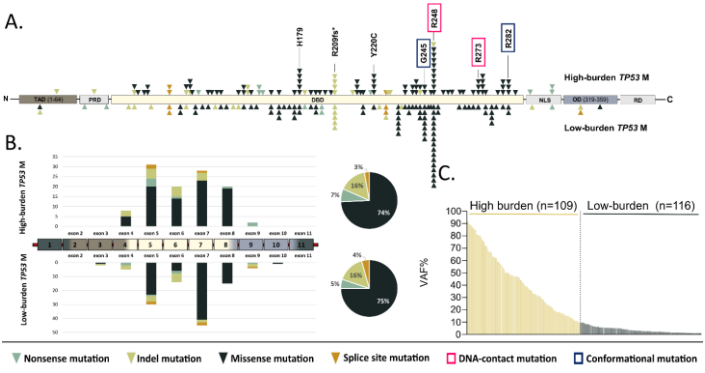


***Figure 3. Distribution and type of TP53 mutations along the TP53 gene and protein in the high-VAF and low-VAF TP53 mutation context.*** (A) Mutational distributions along the p53 protein. Each triangle represents an individual TP53 mutation with a colour referring to mutation type. (B) Mutational distributions along the coding sequence of the TP53 gene with pie charts showing the frequency of each mutational type. (C) VAFs of TP53 mutations. Each column represents the VAF of an individual TP53 mutation. (Abbreviations: DBD, DNA-binding domain. M, mutation; OD, oligomerisation domain; PRD, proline-rich domain; TAD, transactivation domain.)

### *4.1.4. Deletion of 17p region (del(17p)) and TP53 mutations*

Del(17p) status was available for 795 patients, with the deletion detected in 9.2% (73/795) of cases (Figure 4). Among these, 75.3% (55/73) also carried a *TP53* mutation (12 low-burden and 43 high-burden), consistent with biallelic *TP53* disruption. Conversely, 39.9% (55/138) of *TP53*-mutated patients harbored a concomitant del(17p). The frequency of 17p deletion was significantly higher in patients with high-burden *TP53* mutations compared to those with low-burden variants (52% vs. 22%, p = 0.0007). The majority of patients with isolated low-burden *TP53* mutations (78.2%, 43/55) lacked del(17p) (Figure 4).

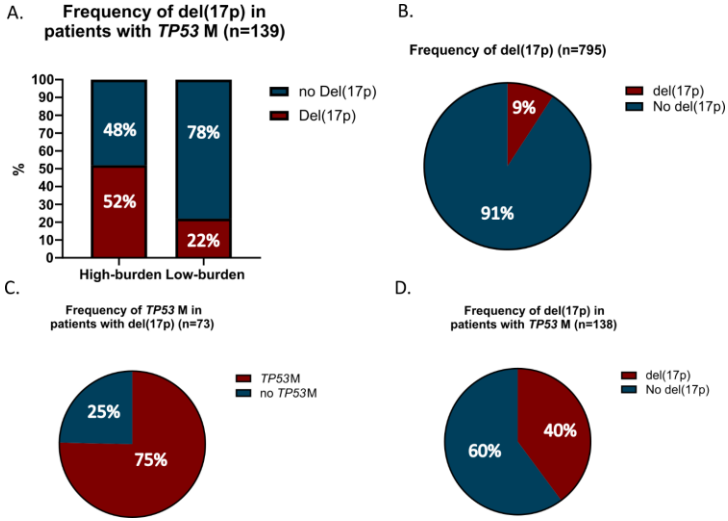


***Figure 4. Frequency and distribution of del(17p) in the cohort.*** (A) Frequency of del(17p) in the high-VAF and low-VAF *TP53* mutation context. (B) Frequency of del(17p) in the cohort, and in patients harbouring *TP53* mutation (D). (C) Frequency of *TP53* mutations in patients harbouring del(17p).

### *4.1.5. Imunoglobulin heavy-chain variable region gene mutational status*

IGHV mutational status was available for 792 patients, distributed as follows: mutated (IGHV-M) in 39.3% (311/792), borderline (IGHV-B) in 5.3% (42/792), and unmutated (IGHV-U) in 55.4% (439/792). *TP53* mutations were significantly more frequent in patients with IGHV-U compared to IGHV-M ($p = 0.0009$). Most patients carrying either low-burden or high-burden *TP53* mutations had IGHV-U status (70.6% and 67.4%, respectively), whereas IGHV-U was less common in patients without *TP53* mutations (52.7%).

### *4.1.6. Clinical outcomes of CLL patients*

Considering treatment-free survival (TFS), patients with high-burden ($n = 46$) or low-burden ($n = 28$) *TP53* mutations showed significantly shorter TFS compared to wild-type *TP53* cases ($n = 431$) (high burden vs. wt: $p < 0.0001$; low burden vs. wt: $p = 0.0012$). We observed no significant differences in TFS between patients harbouring high-burden and low-burden mutations ($p = 0.9778$) (Figure 5). Regarding time to first treatment (TTFT), both high-burden ($n = 43$) and low-burden ($n = 26$) mutation carriers had significantly higher treatment initiation rates than wild-type *TP53* patients ($n = 407$) (high burden vs. wt: $p < 0.0001$; low burden vs. wt: $p = 0.0031$). Similar to TFS, no significant differences were detected between high- and low-burden mutations ($p = 0.6993$) (Figure 5).

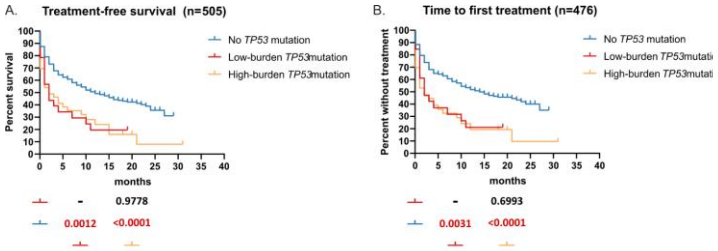


***Figure 5. TFS (A) and TTFT (B) computed as time (months) from sample collection.*** p values are represented in the tables below the panels. Abbreviations: TP53M, *TP53* mutation;

When incorporating IGHV mutational status patients with IGHV-U and *TP53* mutations exhibited significantly shorter TFS and TTFT compared with wild-type *TP53* patients, irrespective of IGHV status.

## *4.2. Copy number analysis of MCL patients treated with targeted therapies*

### *4.2.1. Clinical data*

Following conventional treatment, all MCL patients subsequently received covalent BTKi therapy, with most (n = 11) receiving ibrutinib and one patient (MCL7) receiving acalabrutinib. The median time to progression on BTKi therapy was 20.5 months (2–87 months). Upon progression, patients were treated with venetoclax, with a mean interval of 29.9 days between BTKi progression and venetoclax initiation. Venetoclax was administered as monotherapy in 67% of patients (8/12) and in combination with other agents in 33% (4/12). Following a median treatment duration of 20 months, disease progression occurred in 58% of patients (7/12). Of these, five patients died within a median of 24 days after progression.

### *4.2.2. Evaluation of copy number alterations (CNA)*

LcWGS was performed on 21 samples to evaluate genome-wide copy number profiles of sequential MCL cases (Figure 6). Virtually all samples harbored at least two arm-level CNAs (range: 2-21). Deletions were more common, detected in 90.5% of samples (19/21), with a median of four deletions per case (Figure 7). In comparison, arm-level gains occurred in 71.4% of samples (15/21), with a median of one amplification per case.

### *4.2.3. Comparison of BTKi early versus late progressor patients*

The cohort was stratified into BTKi early and late progressors based on time to progression, defined as time from BTKi initiation to first documented progression. Early progressors were those who developed clinical signs of progression within one year (range: 2–7 months). For comparison, diagnostic samples were analyzed when available, in two

cases where such material was lacking, pre–targeted treatment samples were used. Arm-level deletions affecting the long arm of chromosome 6 were detected in four out of seven patients in the late progressor cohort, whereas this alteration appeared in only one case among early progressors. In the early progressor group (n = 5), the most frequently altered cytobands (observed in three cases each) included 1p21.2, 9q34.3, 11q14.2, 11q14.3, 11q22.2, 11q22.3, and 13q14.2. These regions encompass genes previously implicated in ibrutinib resistance, such as *NOTCH1*, *TRAF2*, *BIRC2*, *BIRC3*, and *ATM*. Of these cytobands, 1p21.2 (*S1PR1*) and 13q14.2 (*FNDC3A*) were affected exclusively by deletions. CNAs affecting cytobands 9q34.3 (*NOTCH1*, *TRAF2*) and 11q14.2 were present only in the early progressor group.

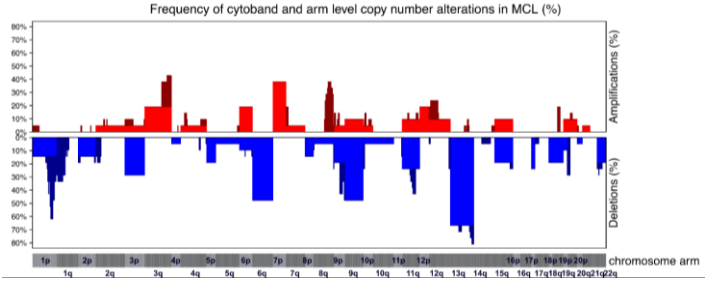


***Figure 6. Frequency histogram of copy number variations at cytoband and arm resolution.*** The diagram illustrates the frequency of copy number variations at both cytoband and arm resolution. Arm-level alterations are depicted using lighter shading, while cytoband-level alterations are depicted using darker bars. Only copy number alterations that encompassed at least 50% of the chromosomal arm were classified as "arm-level changes."

Deletions affecting the long arm of chromosome 13 were identified comparably in the early and late progressor group (three out of five early progressor versus five out of seven late progressor), highlighting that, despite its high prevalence, its contribution to ibrutinib resistance is unlikely (Figure 7).

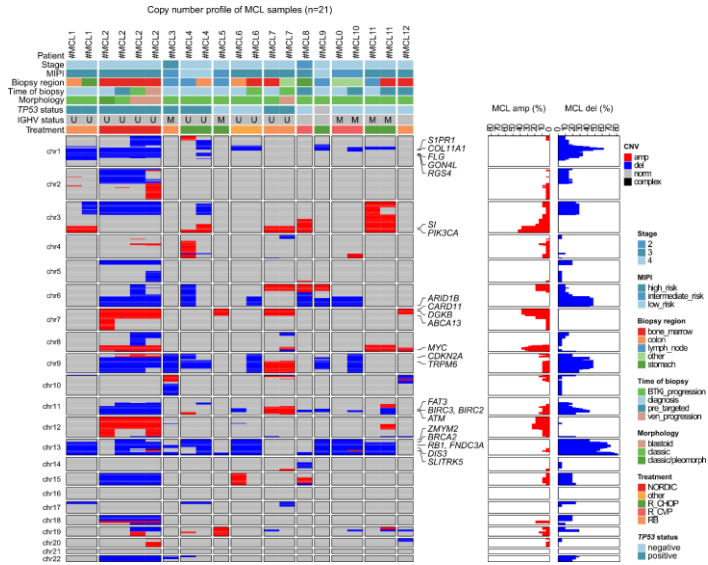


***Figure 7. Copy number profiles of all MCL samples included in the study.*** The upper panel summarizes clinicopathological features, where disease stage, MIPI score, *TP53* status, IGHV status, and treatment history are patient-related, while biopsy site, biopsy timing, and morphology refer to the individual samples. Genes located in regions with CNAs present in at least 35% of samples are shown on the right side of the heatmap.

### *4.2.4. Comparison of venetoclax responder versus nonresponder patients*

The cohort included nine venetoclax responders and three non-responders. Two of the three non-responders exhibited complete loss of chromosome 9, compared with only one case (1/9) in the responder group. In both non-responders with del(9p), the deletion extended across the *CDKN2A* coding region. Among responders, a total chromosome 9 deletion was detected in one patient (MCL4), and a focal 9p21.3 deletion involving *CDKN2A* was identified in another (MCL9). In two of the three non-responders, deletions were detected

at cytobands 9q34.3 and 22q11.23, encompassing the coding regions of *NOTCH1*, *TRAF2*, *BCR*, and *KIAA1671*. Recurrent amplifications, observed in at least two non-responders, involved cytobands 7p22.2, 7p21.2, and 7p12.3, affecting genes such as *CARD11*, *DGKB*, and *ABCA13*. While deletions on chromosome 13q emerged with similar frequency in both early and late progressor BTKi patients, the ratio substantially varied regarding venetoclax responsiveness. None of the non-responders carried arm-level 13q deletions, whereas this alteration was the most frequent among responders (6/9). In contrast to the frequent deletions, amplifications were rare, detected in three of nine cases, and involved a large segment of chromosome 3q (3q25.31–3q29), including the *PIK3CA* coding region.

#### *4.2.5. Evolution of copy number profile of MCL during targeted therapy*

Serial tissue samples were collected from five patients treated with BTKi and venetoclax sequentially. A comparison of CNA counts between pre- and post-treatment samples ($n = 21$) revealed a significantly higher number of CNAs in post-treatment samples ($p = 0.039$; Wilcoxon test; data not shown). During chemo-immunotherapy, copy number profiles of serial samples ($n = 3$ pairs) revealed both overlapping alterations and dynamic changes at relapse, with new variants emerging and some preexisting alterations diminishing. Newly acquired arm-level alterations were predominantly deletions, while amplifications were observed in only one case. Comparison of diagnostic and BTKi relapse samples ($n = 3$ pairs) revealed the emergence of new variants at relapse, predominantly deletions. Although no cytoband was altered in all relapsed samples, a few were affected in two samples, encompassing genes previously implicated in MCL. Notably, novel loss of 8p12–8p23.2 was observed in two of three relapsed samples, including the coding region of *DLC1*, a key regulator of cell adhesion that has been reported as signifficantly mutated in MCL.

#### 4.2.6. Temporal analysis of clonal evolution in double-resistant patient undergoing morphological shift

The patient exhibited a complex, branching clonal evolution, with some alterations persisting while others appeared or disappeared across relapses and

treatment changes (Figure 8). In diagnostic samples, lcWGS revealed a complex genomic landscape with multiple CNAs that were maintained throughout the disease course. At first relapse following chemo-immunotherapy, preexisting amplifications on the long arms of chromosomes 7 and 12 diminished, while new gains emerged on the short arm of chromosome 9. Like most newly acquired CNAs, these amplifications persisted throughout the disease course. In addition, novel large deletions were identified on chromosomes 11 and 13: del(11)(q11–q13.2) and del(13)(q12.11–q34). Concurrent with the morphological switch, new deletions and amplifications appeared at the time of ibrutinib relapse and persisted in the subsequent sample collected at venetoclax relapse. Notably, these CNAs included deletions affecting the coding regions of *SMARCA4* [del(19)(p13.3–q13.11)], a key component of the SWI-SNF chromatin remodeling complex, as well as *DLC1* [del(8)(p23.2–q11.1)] (Figure 8). In the final sample acquired from the time of venetoclax relapse, lcWGS revealed newly emerging CNAs, with amplifications being the predominant alteration. These included amplification of the long arm of chromosome 2, recurrence of amp(12)(q21.31–q24.31) previously observed in the diagnostic sample, and gain of the long arm of chromosome 20. In addition to amplifications, a novel deletion affecting the long arm of chromosome 5 del(5)(q14.3–35.3) was identified (Figure 8). In addition to the appearance of novel CNAs, venetoclax treatment successfully eliminated major deletions present in the diagnostic and previous relapsed samples, respectively: del(2)(p24.1–13.1) and del(9)(q31.3–34.3). Similarly, several deletions acquired during chemo-immunotherapy or ibrutinib treatment were eliminated during BCL2 inhibitor therapy (Figure 8).

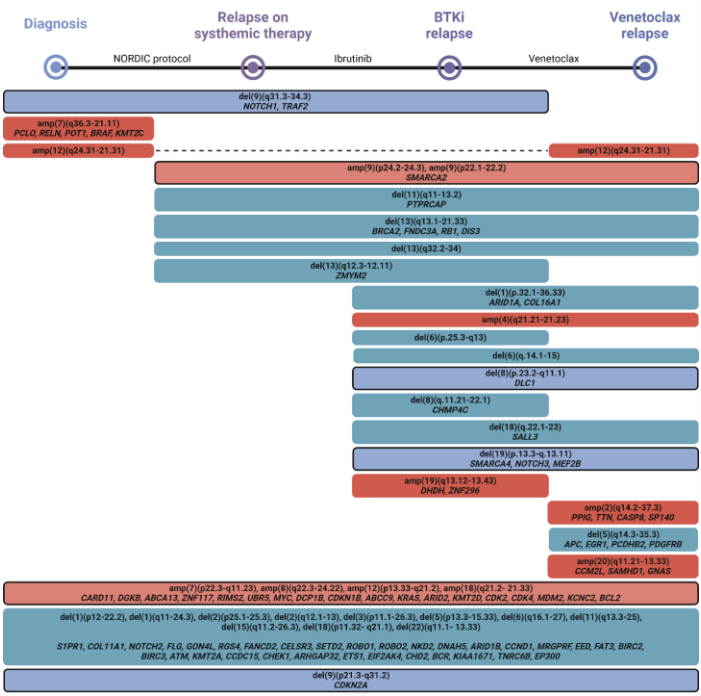


***Figure 8. Copy number profile of patient MCL2.*** Red bars indicate amplifications, while blue bars represent deletions. Bar length reflects the presence of CNAs relative to the time of diagnosis, first relapse, BTKi relapse, or venetoclax relapse. Genes within the corresponding cytobands are shown below each bar. Bordered bars highlight chromosomal regions harboring potentially important genes involved in therapy resistance, including *CARD11*, *CDKN2A*, and *DLC1*.

## 5. CONCLUSIONS

Novel findings of my thesis:

- Sole low-burden *TP53* mutations are frequent, representing 39% of all *TP53*-mutated cases. Since most of these patients (approximately 80%) lacked concurrent del(17p), the identification of these cases is of paramount importance.
- Our findings confirm that NGS is sufficiently sensitive to reliably detect low-burden *TP53* variants at 5–10% VAF. Notably, in our cohort, variants were consistently detectable down to 2% VAF, underscoring the need for each laboratory to establish and validate its own reporting threshold.
- To the best of our knowledge, this study provides the largest dataset examining the clinical impact of low-burden *TP53* mutations while accounting for IGHV status in CLL. We observed significant differences in TTFT and TFS between patients harboring low-burden *TP53* variants vs wild-type patients. By extending our analysis with IGHV status, synergy was detected between unmutated IGHV status and the presence of low-burden or high-burden *TP53* mutations, with patients harbouring both markers having significantly lower TFS and TTFT.
- Our findings support the idea that alterations in the noncanonical NF-κB pathway contribute to BTKi resistance in MCL. In early progressors, frequent copy number changes affecting *TRAF2*, *BIRC2*, and *BIRC3* were observed, supporting the role of the alternative NF-κB pathway in reduced ibrutinib sensitivity.
- Our data indicate that novel loss of *DLC1* may represent an unrecognized mechanism of BTKi resistance in MCL, as recurrent deletion of 8p12–8p23.2 could disrupt this key regulator of cell migration and proliferation, potentially enabling BTK-independent survival pathways and contributing to therapy resistance in MCL.
- Loss of *CDKN2A* may contribute to primary venetoclax resistance in MCL. Early progressors in our cohort frequently exhibited 9p21.3 deletions affecting *CDKN2A*, highlighting its potential central role in mediating resistance.

- NF-κB pathway alterations broadly impact targeted therapy efficacy. Early-progressor patients on venetoclax displayed deletions of *TRAF2/NOTCH1* or amplification of *CARD11*, indicati51ng constitutive NF-κB2/NF-κB1 activation.

## 6. BIBLIOGRAPHY OF THE CANDIDATE'S PUBLICATIONS

Publications related to the PhD thesis:


1. **Tamás László**, László Imre Pinczés, Bence Bátai et al. Resistance mechanisms and clonal dynamics in mantle cell lymphoma treated with sequential BTKi and venetoclax therapy. Journal of Pathology, 2025 DOI: 10.1002/path.6434. D1

2. **László T**, Kotmayer L, Fésüs V, et al. Low-burden TP53 mutations represent frequent genetic events in CLL with an increased risk for treatment initiation. J Pathol Clin Res. 2024 Jan;10(1):e351. doi: 10.1002/cjp2.351. Epub 2023 Nov 21. PMID: 37987115; PMCID: PMC10766018. D1


Other publications:


1. Sayam Ghosal, Bernadett R Bodnár, Brachyahu M Kestecher, Ákos Nagy, **Tamás László**, Bora Yilmaz, Yixuan Zeng, Adrienn Szabó, Csaba Bödörr, Edit I Buzás, Xabier Osteikoetxea, Revolutionizing therapeutics: unleashing the power of extracellular vesicles for disease intervention, Current Opinion in Physiology,, vol 43. (2025) 100815

2. **László, Tamás** et al. “A mérhető reziduális betegség lehetőségei a hematológiai malignitásokban” The clinical potential of measurable residual disease in hematological malignancies. Magyar onkologia vol. 68,4 (2024): 364.

3. **László, Tamás** ; Csacsovszky, Ottó ; Bödör, Csaba Új megközelítések a B-sejtes lymphomák kezelésében KLINIKAI ONKOLÓGIA 11 : 2 pp. 139-148. , 10 p. (2024)

4. Bátai B, Kiss L, Varga L, Nagy Á, Househam J, Baker AM, **László T**, et al. Profiling of Copy Number Alterations Using Low-Coverage Whole-Genome Sequencing Informs Differential Diagnosis and Prognosis in Primary Cutaneous Follicle Center Lymphoma. Mod Pathol. 2024 May;37(5):100465. doi: 10.1016/j.modpat.2024.100465. Epub 2024 Mar 7. PMID: 38460675; PMCID: PMC11092316.

5. Bödör, Csaba ; Alpár, Donát ; Bátai, Bence ; **László, Tamás**; A hazai onkohematológiai kutatás szolgálatában: A Molekuláris Onkohematológia Kutatócsoport első tíz éve; MAGYAR ONKOLÓGIA 67 : 3 pp. 260-265. , 6 p. (2023)

6. Kotmayer, L.; **László, T**.; Mikala, G.; et al. Landscape of BCL2 Resistance Mutations in a Real-World Cohort of Patients with Relapsed/Refractory Chronic Lymphocytic Leukemia Treated with Venetoclax. Int. J. Mol. Sci. 2023, 24, 5802. https://doi.org/10.3390/ijms24065802

7. Takács F, Kotmayer L, Czeti Á, Szalóki G, **László T**, Mikala G, Márk Á, Masszi A, Farkas P, Plander M, Weisinger J, Demeter J, Fekete S, Szerafin L, Deák BM, Szaleczky E, Sulák A, Borbényi Z, Barna G. Revealing a Phenotypical Appearance of Ibrutinib Resistance in Patients With Chronic Lymphocytic Leukaemia by Flow Cytometry. Pathol Oncol

Res. 2022 Sep 21;28:1610659. doi: 10.3389/pore.2022.1610659.

8. Bödör*, Kotmayer*, **László**, Takács, et al. Screening and monitoring of BTKC481S mutation in a real-world cohort of patients with relapsed/refractory chronic lymphocytic leukemia during ibrutinib therapy, 2021, BJH

9. **László, Tamás** ; Kotmayer, Lili ; Alpár, Donát ; Bödör, Csaba Venetoclax-rezisztencia krónikus lymphocytás leukémiában HEMATOLÓGIA-TRANSZFUZIOLÓGIA 54 : 3 pp. 143-151. , 9 p. (2021)